Large-scale numerical investigations of the antiferromagnetic Heisenberg icosidodecahedron

Jörg Ummethum[a], Jürgen Schnack[a,*], Andreas M. Läuchli[b]

[a]*Dept. of Physics, Bielefeld University, P.O. box 100131, D-33501 Bielefeld, Germany*
[b]*Inst. f. Theoretische Physik, Innsbruck University, Technikerstr. 25, 6020 Innsbruck, Austria*

Abstract

We present up to date investigations of the antiferromagnetic Heisenberg icosidodecahedron by means of the Density Matrix Renormalization Group method. We compare our results with modern Correlator Product State as well as Lanczos calculations.

Keywords: Molecular Magnetism, DMRG, Frustration
PACS: 75.50.Xx, 75.10.Jm, 78.70.Nx

1. Introduction

Thanks to advanced chemical strategies there exist several chemical realizations of icosidodecahedral magnetic molecules: $Mo_{72}Fe_{30}$[1], $W_{72}Fe_{30}$[2] (both $s = 5/2$), $Mo_{72}Cr_{30}$[3] ($s = 3/2$), $Mo_{72}V_{30}$[4, 5], and $W_{72}V_{30}$[6] (both $s = 1/2$). These molecules are some of the largest magnetic molecules synthesized to date [7]. Icosidodecahedral magnetic molecules are of special interest because they are highly symmetric, frustrated, exist with different spin quantum numbers, and are a kind of finite-size version of the Kagomé lattice antiferromagnet [8]. Fig. 1 shows the structure of the icosidodecahedron. It is an Archimedian Solid with 12 pentagons and 20 triangles, which means that it is geometrically frustrated [9].

Experimental investigations of these molecules are in most cases measurements of the susceptibility as a function of temperature [1, 2, 3, 4, 5, 6] or magnetic field [10, 11], or magnetization as a function of the applied magnetic

---

*corresponding author
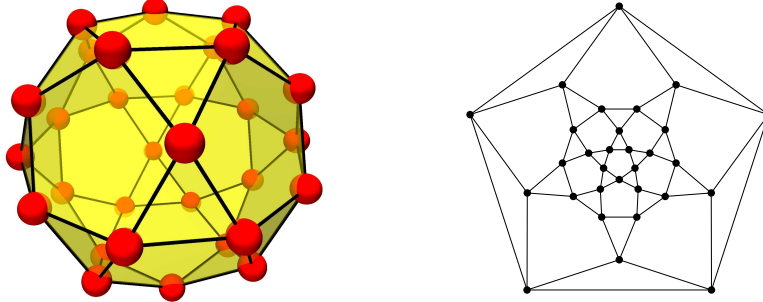*Email address:* jschnack@uni-bielefeld.de (Jürgen Schnack)

Figure 1: Structure of the icosidodecahedron: the black bullets correspond to the spin positions and the lines to interaction paths between them. The right part of the figure shows the two-dimensional projection.

field [1, 11, 12]. These experimental investigations show that the icosidodecahedral magnetic molecules are antiferromagnetic with a nonmagnetic ground state. Other experimental techniques that were applied to these molecules are NMR and μSR [13, 14, 15], INS [16], diffuse (elastic) neutron scattering, as well as specific heat measurements [17].

These molecules are usually modeled using a simple Heisenberg model [1, 2, 3, 4, 6, 16, 17, 18, 19, 20, 21, 22, 23]. Anisotropic terms were considered in Refs. [22, 24]. Bond disorder and distortions (i.e., more than just one exchange constant in the Heisenberg Hamiltonian) were investigated in Refs. [10, 23]. However, since the icosidodecahedral molecules comprise $N = 30$ spins, the numerical exact calculation of $T = 0$ properties is possible only for the $s = 1/2$ case [8, 25, 26]. Quantum Monte Carlo suffers from the negative-sign problem so that small temperatures are not feasible [3, 4, 6]. Thermodynamical properties at $T > 0$ can for $s = 1/2$ also be calculated quasi-exactly using the finite-temperature Lanczos method [21, 23, 27]. For $s > 1/2$, approximations are needed. For $s = 3/2$ and $s = 5/2$ systems, the classical Heisenberg model was used together with efficient classical Monte Carlo algorithms [1, 2, 10, 18, 19, 22, 28]. However, such an approximation is inappropriate at very low temperatures. The rotational band approximation was used in Refs. [1, 12, 16, 17, 20, 29, 30]. Although being a quantum mechanical approximation it misses important features of frustrated systems such as magnetization jumps and plateaus or low-lying singlets in the spectrum [25]. Another approximation applied to the icosidodecahedron is spin-

2

wave theory [20, 24]. However, as for the rotational band and the classical approximation, it is not clear how accurate this approximation is.

It has to be emphasized here that although there exist many theoretical studies on the icosidodecahedron for $s > 1/2$, accurate numerical calculation for the *full* Heisenberg model are very rare. The Density Matrix Renormalization Group (DMRG) method allows for treating the full Heisenberg Hamiltonian but in a reduced Hilbert space [31, 32]. It relies on a controlled truncation of the Hilbert space and allows for the estimation of the accuracy so that it seems to be suited for these systems. In Ref. [33] the DMRG method has already been applied to the Heisenberg icosidodecahedron with $s = 5/2$. However, only up to $m = 120$ density matrix eigenstates were used, so that the accuracy of the results is rather limited for such a complicated system with a geometry that is not favorable for the DMRG method.

In this article we apply the DMRG method to the antiferromagnetic Heisenberg icosidodecahedron. We focus on the calculation of the lowest energies in subspaces of total magnetic quantum number M which allow for a calculation of the $T = 0$ magnetization curve and also gaps which might be of importance for spectroscopic methods such as, e.g., Inelastic Neutron Scattering (INS). These results are compared with very recent variational Monte Carlo calculations using correlator product states (CPS) by Neuscamman and Chan in Ref. [34]. Finally, for the case $s = 1/2$ we also calculate the dynamical correlation function $S^z_{\text{loc}}(\omega)$ using the Dynamical DMRG (DDMRG) [35].

2. DMRG results

The DMRG technique is best suited for open one-dimensional chain systems but can be applied to systems with an arbitrary geometry. The icosidodecahedron can be viewed as a two-dimensional lattice on a sphere (similar to the Kagome lattice, see [8]), i.e., with periodic boundary conditions. This means that the convergence is much slower than in one-dimensional systems [33]. But since DMRG is a variational method, it is clear that the ground state – or the lowest energy in a subspace – is the better the lower the corresponding energy is. Also, the truncated weight Δw offers the possibility to judge the quality of the results and an extrapolation to zero truncated weight (or $m \to \infty$) might be possible.

For the investigations throughout this article we employ the Heisenberg

3

Hamiltonian

$$\underset{\sim}{H} \;\; = \;\; J \sum_{i<j} \underset{\sim}{\vec{s}}_i \cdot \underset{\sim}{\vec{s}}_j + g\,\mu_B\,B \sum_i \; \underset{\sim}{s}_i^z \tag{1}$$

with antiferromagnetic isotropic nearest neighbor exchange J only.

2.1. Numbering of the spins

When DMRG is applied to spin systems that are not one-dimensional, the usual way is to map the system on a one-dimensional chain with long-range interactions, i.e., to number the spins of the lattice [36]. However, if not very simple systems such as, e.g., ladders are investigated, it is not clear, which numbering is best suited. Such a problem also occurs, when DMRG is applied in the context of quantum chemistry, where models similar to the Hubbard model with long-range interactions appear and the ordering, i.e., the numbering of the orbitals is relevant [37, 38, 39, 40, 41]. Since long-range interactions diminish the accuracy of DMRG (cf. Ref. [42]) it is clear that a good ordering needs to minimize such long-range interactions.

We have tested several numberings for the icosidodecahedron. The resulting coupling matrices J_{ij} are shown in Fig. 2. The numbering used by Exler and Schnack in an earlier investigation [33] (see top left of Fig. 2) gives a very regular "interaction pattern" with rather-short-ranged interactions, but the "periodic boundaries", i.e., interactions between the first and the last spins, are clearly not optimal for the DMRG algorithm with two center sites. As proposed in Ref. [37], we have used a variant of the reverse Cuthill-McKee algorithm [43, 44], the RCMD algorithm, which aims to number the vertices such that the bandwidth of the matrix is minimized. We have also used the Sloan algorithm [45] which minimizes the "envelope size", i.e., the sum of the "row bandwidths". (The bandwidth is the maximum of the row bandwidths.) We have used these algorithms as implemented in Mathematica [46]. The figure also shows an unoptimized numbering for comparison.

The results of DMRG calculations (using the ALPS DMRG code [47]) for the different spin numberings are shown in Fig. 3. We have calculated the ground state energy of the $s = 1/2$ icosidodecahedron with an increasing number of kept density matrix eigenstates (m) so that the convergence can be investigated and a comparison with the exact ground state energy (see Ref. [8]) is possible. One can see that the different optimized numberings (Exler/Schnack, RCMD, and Sloan) give almost identical results whereas the unoptimized numbering gives much worse results. These results show
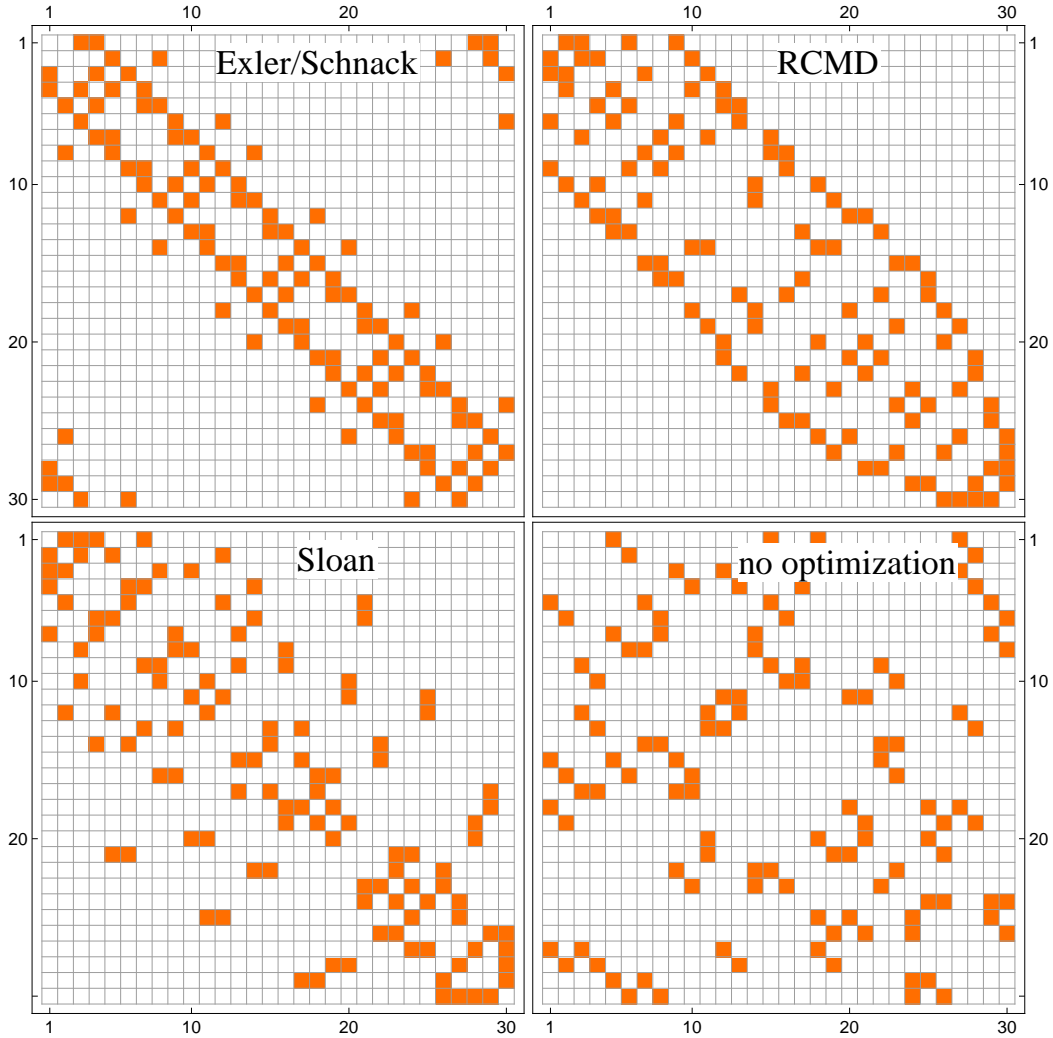
Figure 2: Depiction of the coupling matrix (J_{ij}) for four different numberings of the vertices of the icosidodecahedron. Nonzero entries are denoted by the orange squares. Top left: numbering according to Exler and Schnack (see Ref. [33]); top right: result of the RCMD algorithm; bottom left: result of the Sloan algorithm; bottom right: unoptimized numbering.

that a "good" numbering of the spins is absolutely essential if the DMRG method is applied to a spin system with a complicated structure. For the following results we have always used the numbering as proposed by Exler and Schnack.
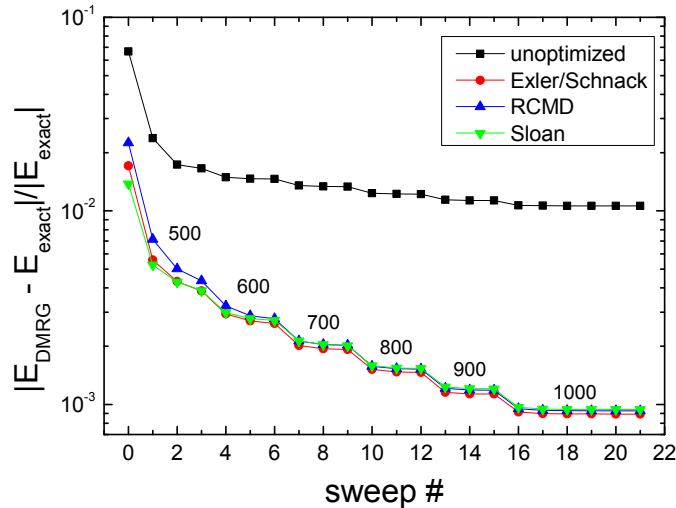
Figure 3: DMRG results for different numberings (see Fig. 2) of the spins sitting on the vertices of the icosidodecahedron. The plot shows the error in the ground state energy as obtained by DMRG and as a function of the DMRG sweep. The numbers above the symbols denote the number of kept density matrix eigenstates for the sweep.

2.2. Lowest energy eigenvalues and magnetization curves

As a next step we have calculated the lowest energies in the M subspaces for the icosidodecahedron with $s > 1/2$ using DMRG. The results for the $s = 1/2$ system already showed that DMRG is able to produce very accurate results for this system with relative errors smaller than 10^{-3}.

Fig. 4 shows the lowest energy eigenvalues in the subspaces of total magnetic quantum number M for the icosidodecahedron with $s = 1$ and $s = 3/2$ as obtained by DMRG and – for the large-M subspaces ($M > 18$ for $s = 1$ and $M > 33$ for $s = 3/2$) – Lanczos calculations. We have used up to $m = 2500$ density matrix eigenstates for the $s = 1$ case and up to $m = 2000$ for the $s = 3/2$ case. The largest truncated weight within a sweep is of the order of $7 \cdot 10^{-4}$ for the $M = 0$ subspace of the $s = 1$ icosidodecahedron and of the order of $4 \cdot 10^{-4}$ for the $s = 3/2$ case. That the truncated weight for the $s = 1$ icosidodecahedron is larger than for $s = 3/2$ although more states have been used for $s = 1$ indicates that it cannot be reliably used for a quantitative estimate of the error. The reason for this behavior might be that the results are not yet fully converged for the value of m that we have used, although we have carried out up to 60 sweeps for the calculations.

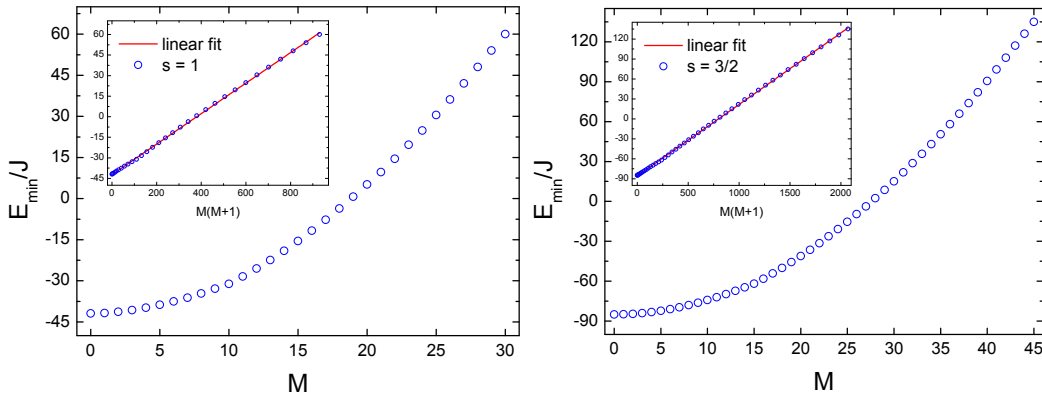The rotational band model predicts a behavior of the form $E_{\min}(M) =$

Figure 4: Lowest energy eigenvalues in the subspaces of total magnetic quantum number M as obtained by DMRG calculations. The eigenvalues for the smallest subspaces, i.e., for large M, were calculated using the Lanczos algorithm (calculations performed by J. Schnack, private communication). For the DMRG calculations, the ALPS DMRG code was employed [47]. For the $s = 1$ system we have kept $m = 2500$ density matrix eigenstates in all DMRG calculations. For the $s = 3/2$ system we have kept $m = 2000$ states for the subspaces up to $M = 4$, $m = 1500$ states for the subspaces $5 \leq M \leq 23$, and 1000 states for the subspaces $M > 23$.

$aM(M + 1) + b$, i.e., a parabolic dependence [12]. The insets of Fig. 4 show that this is a good approximation for the energy eigenvalues of the full Heisenberg model. The simple rotational band approximation predicts a proportionality constant of $a = 0.1$. The linear fits as shown in the insets give the results $a = 0.111$ for $s = 1$ and $a = 0.108$ for $s = 3/2$, very close to the simple rotational band approximation. However, if one uses these (DMRG) data to calculate the zero-temperature magnetization curve, it becomes clear that there are some crucial deviations from the ideal parabolic dependence. If there was an ideal parabolic dependence, the resulting magnetization curve would consist of steps with constant widths. Fig. 5 shows the resulting zero-temperature magnetization curves as calculated using the DMRG data. Again, the exact diagonalization data for $s = 1/2$ is taken from Ref. [8].

One can see, that the magnetization curves do not consist of steps with constant widths. There are some anomalies as expected for frustrated systems. The plateaus at $\mathcal{M}/\mathcal{M}_{\text{sat}} = 1/3$ are clearly visible. The magnetization jumps due to the independent magnons [26] are also visible. Since the jump has a height of $\Delta M = 3$, it is clear that this effect vanishes for $s \to \infty$ in the plot because the magnetization is normalized by the saturation magnetization $\mathcal{M}_{\text{sat}} = 30g\mu_B s$. For $s \to \infty$, the classical result, i.e., a strictly
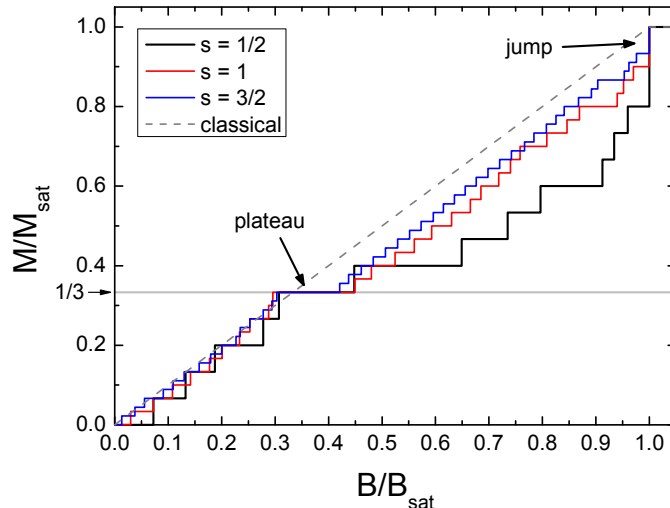
Figure 5: Zero-temperature magnetization curves of the icosidodecahedron as obtained by DMRG ($s = 1$, $s = 3/2$) calculations (cf. Fig. 4). The data for $s = 1/2$ is taken from Ref. [8]. The plot also shows the classical result [19]. The data is normalized to the saturation field and magnetization.

linear magnetization curve [19], will be reached. On the contrary, the plateau seems to be very stable when increasing s. A similar behavior has already been found for the cuboctahedron, compare Ref. [8].

For the cases $s = 2$ and $s = 5/2$ we have calculated the lowest energy eigenvalues only in some M subspaces, including those subspaces that are relevant for the calculation of the plateau width. We have kept $m = 2000$ density matrix eigenstates for these calculations. The plateau is clearly visible, even for $s = 5/2$. However, it is not clear if these plateaus can be measured in experiments, since for $s = 1/2$ the plateau disappears rather quickly with increasing temperature [21]. Fig. 7 shows the plateau widths for different s as obtained by the DMRG calculations (cf. Fig. 6) and the exact diagonalization for $s = 1/2$ [8]. The left part of Fig. 7 shows an extrapolation to $s \to \infty$ using the data for $s > 1/2$. The extrapolated value for the plateau width is 0.013 and not exactly zero but rather close the expected value. It has to be emphasized here that the plateau widths shown in Fig. 7 are approximate values for $s > 1/2$. The accuracy of the results is analyzed in the next subsection.
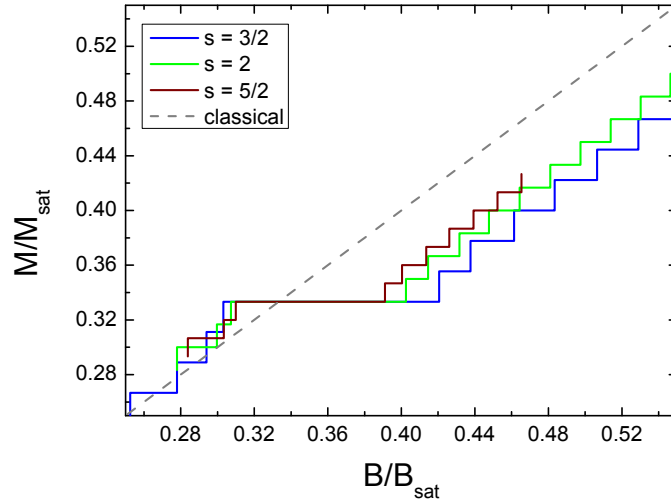
Figure 6: Zero-temperature magnetization curves of the icosidodecahedron for $s = 3/2, 2, 5/2$ as obtained by DMRG calculations (cf. Fig. 4). The plot also shows the classical result [19]. The data is normalized to the saturation field and magnetization.
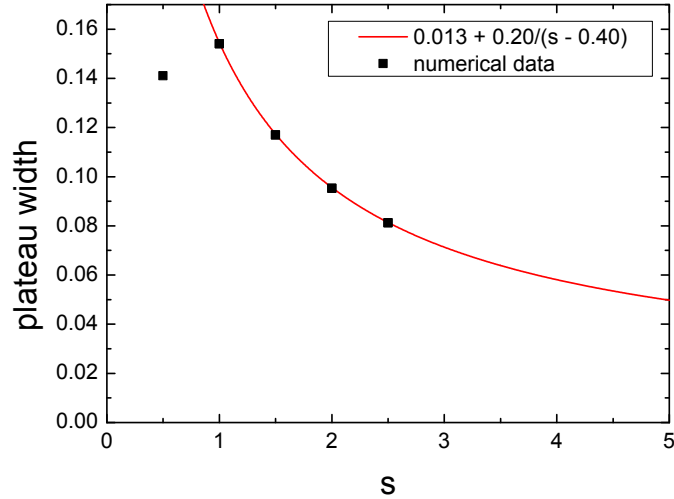

Figure 7: Plateau widths for different s quantum numbers as obtained by DMRG $S > 1/2$ and exact diagonalization $s = 1/2$ calculations. The exact diagonalization values are taken from Ref. [8]. This part of the plot also includes an extrapolation to $s \to \infty$ using the data for $s > 1/2$. The extrapolated value for the plateau width is 0.013.

2.3. Extrapolation to $m \to \infty$ and error estimates

A sensible extrapolation in m (the number of kept density matrix eigenstates) or Δw (truncated weight) is only possible when the results are fully converged for the current m value. Fig. 8 shows the ground state energy and the lowest energy in the $M = 1$ subspace of the $s = 1$ icosidodecahedron as calculated using DMRG for different m values.
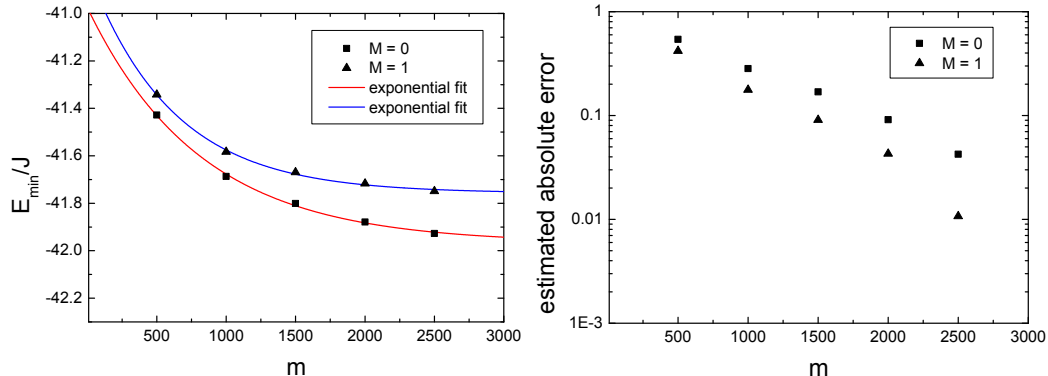

Figure 8: Left: DMRG results for the lowest energy eigenvalues of the $M = 0$ and the $M = 1$ subspace. m denotes the number of kept density matrix eigenstates. The lines are exponential fits to the data. Right: estimated absolute error as a function of m.

An extrapolation with an exponential ansatz yields $E_{\min}^{\text{extra}}(M = 0) = -41.97(2)J$ and $E_{\min}^{\text{extra}}(M = 1) = -41.76(1)J$.[1] In Ref. [33], the results were extrapolated using an ansatz of the form $a + b/m$. However, this ansatz did not work well for our data which is based on much larger m values. The right part of Fig. 8 shows the estimated absolute error, i.e., the difference between the extrapolated energy and the energy value obtained for finite m, as a function of m. For $s > 1$ such an extrapolation was not possible since the production of enough converged energies for different m values is virtually impossible.

Fig. 9 shows the convergence of the width of the $\mathcal{M}_{\text{sat}}/3$ plateau as a function of m. One can see that the plateau width decreases with increasing m so that DMRG seems to overestimate the width of plateau. We find similar effects for $s > 1$, but since the calculations are extremely time-consuming, it was not possible to obtain enough numerical data for a more systematic study

---

[1]The errors given in parenthesis are the standard errors of the fitting procedure.
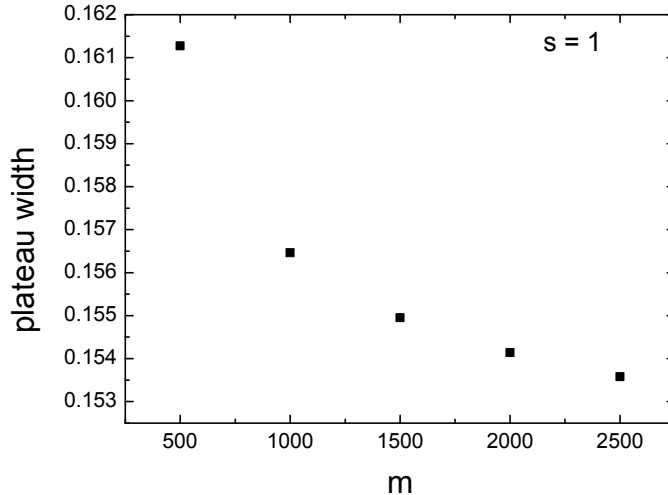
Figure 9: The plateau width of the $s = 1$ icosidodecahedron as a function of the number of density matrix eigenstates that were kept in the DMRG calculations.

of this effect. Looking more carefully at the truncated weights, we find that the DMRG calculations of the lowest energy in the $M = 10s(= \mathcal{M}_{\text{sat}}/(3g\mu_B))$ subspace result in smaller values of the truncated weight than the calculations in the adjacent subspaces with the same m. However, the order of magnitude of the truncated weight is still the same. This indicates that DMRG leads to more accurate results exactly at one-third of the saturation magnetization which has the consequence that the method seems to systematically overestimate the plateau width if one works with the same m value for adjacent M subspaces. However, we estimate that the relative errors in the plateau widths are not larger than approximately 10%.

For many one-dimensional systems DMRG can be considered as a numerically exact method. This is clearly not the case for the icosidodecahedron. Nevertheless, the width of magnetization steps would be accurate if the errors of the energy eigenvalues are approximately the same for adjacent M subspaces. But since the subspace dimensions become smaller for increasing M it is clear that calculations with fixed m are more accurate for the large-M subspaces. However, we suppose that the qualitative features of the magnetization curves as predicted by our DMRG calculations are not altered by these considerations since the order of magnitude of the errors is about the same for energy eigenvalues in adjacent magnetization subspaces.

2.4. Comparison with CPS and previous DMRG results

In this subsection we focus on the $s = 5/2$ case and the comparison to previous results on this system. Fig. 10 shows the ground state energy as a function of the DMRG sweep and as a function of the kept density matrix eigenstates. One can see that even for 2000 kept states and more than 30 sweeps the result is not yet converged. A much larger number of states is needed to get convergence. Also, an extrapolation to $m \to \infty$ is not reliably possible because for that many more sweeps would have to be performed.
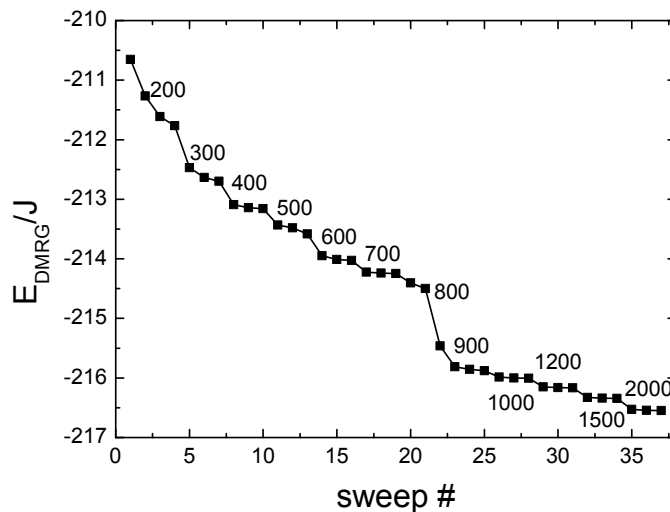

Figure 10: Ground state energy of the $s = 5/2$ icosidodecahedron as a function of the DMRG sweep. The numbers show the retained density matrix eigenstates for the current sweep.

For $m = 2000$ we obtain the value $E_0^{\mathrm{DMRG}} \approx -216.5\,J$. This value can be compared with previous results. The DMRG result of Exler and Schnack for the ground state energy (with $m = 120$) is approximately $-211.1\,J$ [33], a value that is much higher and thus much more imprecise than our result. The very recent result of Neuscamman and Chan using correlator product states in combination with variational Monte Carlo is $-216.3\,J$ [34]. This value is also higher than our DMRG result. Also, the comparison of the lowest energies in the M subspaces that are relevant for the calculation of the plateau width shows that DMRG is – at least for the CPS ansatz used in Ref. [34] – more accurate if enough states are used (see Tab. 1).

M	$E_0^{\mathrm{DMRG}}(M)/J$	$E_0^{\mathrm{CPS}}(M)/J$
24	-158.43	-154.42
25	-153.78	-149.76
26	-147.91	-144.40

Table 1: Comparison of the DMRG energies to the CPS energies. For the DMRG calculations, $m = 2000$ states were kept. The CPS data is taken from Ref. [34].

2.5. Dynamical correlation function for $s = 1/2$

In the following we investigate the dynamical spin correlations of the $s = 1/2$ icosidodecahedron in zero external magnetic field. We focus on the local spin autocorrelation function

$$S_{\mathrm{loc}}^z(\omega) = -\frac{1}{\pi}\mathrm{Im}\langle\mathrm{GS}|S_0^z\frac{1}{\omega - (H - E_{\mathrm{GS}}) + i\eta}S_0^z|\mathrm{GS}\rangle \; . \qquad (2)$$

This quantity is independent of the specific site, since the ground state is found in a non-degenerate, symmetric representation.[2]

We calculate this quantity using two different techniques: i) a continued fraction technique based on the Lanczos Exact Diagonalization (ED) algorithm [48] and ii) a Dynamical DMRG (DDMRG) approach [35].

In Fig. 11 we display the results for $S_{\mathrm{loc}}^z(\omega)$ obtained using both techniques, with excellent agreement for the same broadening $\eta = 0.15J$. The ED results have been obtained using 500 iterations in the continued fraction expansion, while the DDMRG results have been obtained using $m = 2000$ states, which results in very time-consuming calculations. In the DDMRG $\eta = 0.15J$ is fixed during the calculation, while the ED data can replotted using an arbitrary value for η. For completeness we have also added the pole content obtained within the 500 ED iterations.

Turning to the physics of the spectral function, it displays a rather sharp peak at approximately $0.35J$ and a very broad shoulder which then falls off at approximately $2J$. The rotational band approximation predicts a two-peak structure of the dynamical correlation function. This is clearly not the case since the "real" spectrum is much broader and shows only one distinct peak. However, for such a large $s = 1/2$ system, we cannot expect the rotational

---

[2]This is different in some of the ground states realized at finite magnetization, see Ref. [8].
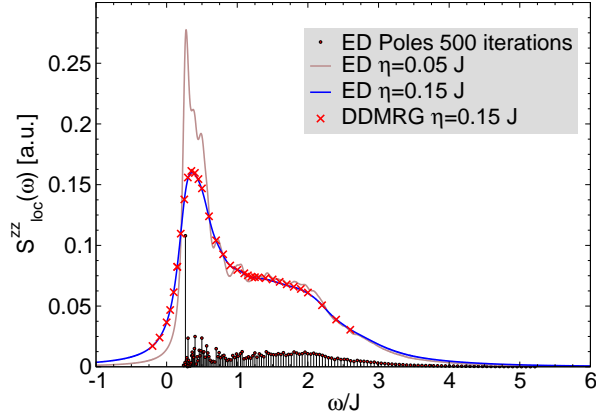
13

Figure 11: The dynamical correlation function $S^z_{loc}(\omega)$ as obtained by ED and DDMRG calculations. In the ED we have used 500 continued fraction iterations whereas in the DDMRG we have used $m = 2000$ and a broadening $\eta = 0.15J$. The agreement between both methods is perfect. The vertical lines show the energies where the simple rotational band model predicts the peaks.

band model to be a good approximation. This approximation is most accurate for small systems with large spin quantum numbers s, compare Ref. [49]. On the contrary, the strong frustration present in the icosidodecahedron results in rather dense spectra of low-lying singlets (even below the lowest triplet), low-lying triplets (even below the lowest quintet) and so on [25, 8] of which the smeared-out dynamical correlation function is a consequence. This behavior is in accord with the experimental INS cross sections obtained for the Keplerate $Mo_{72}Fe_{30}$ with single spin quantum number $s = 5/2$ [16]. It would be very appealing to evaluate the dynamical correlation function for this compound, unfortunately this is virtually impossible at the moment. The main problem is that rather accurate lowest $(S = 0)$ states need to be calculated for the DDMRG method. For the $s = 1$ icosidodecahedron, the estimated error of the ground state energy is already of the order of $0.1J$ using $m = 2000$. This inaccuracy would be too large for a broadening of $\eta = 0.15J$ and either a larger broadening would have to be chosen or more states would be needed. However, keeping more states strongly increases the calculation time and a much larger broadening would probably blur the spectrum too much. Here, a fully optimized and parallelized DDMRG code

would be needed that in addition had to run on a supercomputer.

3. Summary

In this article we report up to date quantum mechanical DMRG calculations for a class of Keplerate magnetic molecules with $s = 1/2, \ldots, 5/2$. We demonstrate that it is possible to obtain lowest energy eigenvalues in orthogonal subspaces and magnetization curves for $T = 0$ with unprecedented accuracy. In addition, using DDMRG as well as Lanczos techniques, we obtained the dynamical correlation function for Keplerates with an intrinsic spin of $s = 1/2$.

Acknowledgment

References

[1] A. Müller, M. Luban, C. Schröder, R. Modler, P. Kögerler, M. Axenovich, J. Schnack, P. Canfield, S. Bud'ko, N. Harrison, Classical and Quantum Magnetism in Giant Keplerate Magnetic Molecules, ChemPhysChem 2 (2001) 517.

[2] A. M. Todea, A. Merca, H. Bögge, T. Glaser, J. M. Pigga, M. L. K. Langston, T. Liu, R. Prozorov, M. Luban, C. Schröder, W. H. Casey, A. Müller, Porous Capsules $\{(M)M_5\}_{12}Fe_{30}^{III}$ (M = Mo^{VI}, W^{VI}): Sphere Surface Supramolecular Chemistry with 20 Ammonium Ions, Related Solution Properties, and Tuning of Magnetic Exchange Interactions, Angew. Chem. Int. Ed. 49 (2010) 514.

[3] A. M. Todea, A. Merca, H. Bögge, J. van Slageren, M. Dressel, L. Engelhardt, M. Luban, T. Glaser, M. Henry, A. Müller, Extending the $\{(Mo)Mo_5\}_{12}M_{30}$ Capsule Keplerate Sequence: A $\{Cr_{30}\}$ Cluster of $S = 3/2$ Metal Centers with a $\{Na(H_2O)_{12}\}$ Encapsulate, Angew. Chem. Int. Ed. 46 (2007) 6106.

[4] A. Müller, A. M. Todea, J. van Slageren, M. Dressel, H. Bögge, M. Schmidtmann, M. Luban, L. Engelhardt, M. Rusu, Triangular Geometrical and Magnetic Motifs Uniquely Linked on a Spherical Capsule Surface, Angew. Chem. Int. Ed. 44 (2005) 3857.

[5] B. Botar, P. Kögerler, C. L. Hill, $[\{(Mo)Mo_5O_{21}(H_2O)_3(SO_4)\}_{12}(VO)_{30}(H_2O)_{20}]^{36-}$: A molecular quantum spin icosidodecahedron, Chem. Commun. (2005) 3138.

[6] A. M. Todea, A. Merca, H. Bögge, T. Glaser, L. Engelhardt, R. Prozorov, M. Luban, A. Müller, Polyoxotungstates now also with pentagonal units: supramoleuclar chemistry and tuning of magnetic exchange in $\{(M)M_5\}_{12}V_{30}$ Keplerates (M = Mo, W), Chem. Commun. 40 (2009) 3351.

[7] D. Gatteschi, R. Sessoli, J. Villain, Molecular Nanomagnets, Oxford University Press, Oxford, 2011.

[8] I. Rousochatzakis, A. M. Läuchli, F. Mila, Highly frustrated magnetic clusters: The kagomé on a sphere, Phys. Rev. B 77 (2008) 094420.

[9] J. Schnack, Effects of frustration on magnetic molecules: a survey from Olivier Kahn until today, Dalton Trans. 39 (2010) 4677.

[10] C. Schröder, R. Prozorov, P. Kögerler, M. D. Vannette, X. Fang, M. Luban, A. Matsuo, K. Kindo, A. Müller, A. M. Todea, Multiple nearest-neighbor exchange model for the frustrated magnetic molecules $\{Mo_{72}Fe_{30}\}$ and $\{Mo_{72}Cr_{30}\}$, Phys. Rev. B 77 (2008) 224409.

[11] U. Kortz, A. Müller, J. van Slageren, J. Schnack, N. S. Dalal, M. Dressel, Polyoxometalates: Fascinating structures, unique magnetic properties, Coord. Chem. Rev. 253 (2009) 2315.

[12] J. Schnack, M. Luban, R. Modler, Quantum rotational band model for the Heisenberg molecular magnet $\{Mo_{72}Fe_{30}\}$, EPL (Europhysics Letters) 56 (2001) 863.

[13] J. K. Jung, D. Procissi, R. Vincent, B. J. Suh, F. Borsa, P. Kögerler, C. Schröder, M. Luban, Proton NMR in the giant paramagnetic molecule $\{Mo_{72}Fe_{30}\}$, J. Appl. Phys. 91 (10) (2002) 7388–7390.

[14] E. Micotti, D. Procissi, A. Lascialfari, P. Carretta, P. Kögerler, F. Borsa, M. Luban, C. Baines, NMR and μSR investigation of spin dynamics in {$Mo_{72}Fe_{30}$} molecular clusters, J. Magn. Magn. Mater. 272-276, Part 2 (2004) 1099.

[15] J. Lago, E. Micotti, M. Corti, A. Lascialfari, A. Bianchi, S. Carretta, P. Santini, D. Procissi, S. H. Baek, P. Kögerler, C. Baines, A. Amato, Low-energy spin dynamics in the giant keplerate molecule {$Mo_{72}Fe_{30}$}: A muon spin relaxation and ^1H NMR investigation, Phys. Rev. B 76 (2007) 064432.

[16] V. O. Garlea, S. E. Nagler, J. L. Zarestky, C. Stassis, D. Vaknin, P. Kögerler, D. F. McMorrow, C. Niedermayer, D. A. Tennant, B. Lake, Y. Qiu, M. Exler, J. Schnack, M. Luban, Probing spin frustration in high-symmetry magnetic nanomolecules by inelastic neutron scattering, Phys. Rev. B 73 (2006) 024414.

[17] Z.-D. Fu, P. Kögerler, U. Rücker, Y. Su, R. Mittal, T. Brückel, An approach to the magnetic ground state of the molecular magnet $Mo_{72}Fe_{30}$, New J. Phys. 12 (2010) 083044.

[18] C. Schröder, H. Nojiri, J. Schnack, P. Hage, M. Luban, P. Kögerler, Competing Spin Phases in Geometrically Frustrated Magnetic Molecules, Phys. Rev. Lett. 94 (2005) 017205.

[19] M. Axenovich, M. Luban, Exact ground state properties of the classical Heisenberg model for giant magnetic molecules, Phys. Rev. B 63 (2001) 100407(R).

[20] O. Waldmann, E-band excitations in the magnetic Keplerate molecule Fe_{30}, Phys. Rev. B 75 (2007) 012415.

[21] J. Schnack, O. Wendland, Properties of highly frustrated magnetic molecules studied by the finite-temperature Lanczos method, Eur. Phys. J. B 78 (2010) 535.

[22] M. Hasegawa, H. Shiba, Magnetic Frustration and Anisotropy Effects in Giant Magnetic Molecule $Mo_{72}Fe_{30}$, J. Phys. Soc. Jpn. 73 (2004) 2543.

[23] N. Kunisada, S. Takemura, Y. Fukumoto, Theoretical study of quantum spin icosidodecahedron ($S = 1/2$) with next-nearest neighbor interactions and analysis of experimental susceptibility for $Mo_{72}V_{30}$, J. Phys.: Conf. Ser. 145 (2009) 012083.

[24] O. Cépas, T. Ziman, Modified Spin-Wave Theory for Nanomagnets: Application to the Keplerate Molecule $Mo_{72}Fe_{30}$, Prog. Theor. Phys. Suppl. 159 (2005) 280.

[25] R. Schmidt, J. Richter, J. Schnack, Frustration effects in magnetic molecules, J. Magn. Magn. Mater. 295 (2005) 164.

[26] J. Schnack, H.-J. Schmidt, J. Richter, J. Schulenburg, Independent magnon states on magnetic polytopes, Eur. Phys. J. B 24 (2001) 475.

[27] J. Jaklic, P. Prelovsek, Lanczos method for the calculation of finite-temperature quantities in correlated systems, Phys. Rev. B 49 (1994) 5065–5068.

[28] S. Torbrügge, J. Schnack, Sampling the two-dimensional density of states $g(E, M)$ of a giant magnetic molecule using the Wang-Landau method, Phys. Rev. B 75 (2007) 054403.

[29] J. Schnack, M. Luban, Rotational modes in molecular magnets with antiferromagnetic Heisenberg exchange, Phys. Rev. B 63 (2000) 014418.

[30] R. Schnalle, A. Läuchli, J. Schnack, Approximate eigenvalue determination of geometrically frustrated magnetic molecules, Condens. Matter Phys. 12 (2009) 331–342.

[31] S. R. White, Density matrix formulation for quantum renormalization groups, Phys. Rev. Lett. 69 (19) (1992) 2863–2866.

[32] U. Schollwöck, The density-matrix renormalization group, Rev. Mod. Phys. 77 (2005) 259–315.

[33] M. Exler, J. Schnack, Evaluation of the low-lying energy spectrum of magnetic Keplerate molecules using the density-matrix renormalization group technique, Phys. Rev. B 67 (2003) 094440.

[34] E. Neuscamman, G. K.-L. Chan, A correlator product state study of molecular magnetism in the giant Keplerate $Mo_{72}Fe_{30}$, arXiv:1203.6883v1 [cond-mat.str-el], 2012.

[35] E. Jeckelmann, Dynamical density-matrix renormalization-group method, Phys. Rev. B 66 (2002) 045114.

[36] E. M. Stoudenmire, S. R. White, Studying Two-Dimensional Systems with the Density Matrix Renormalization Group, Ann. Rev. Cond. Mat. Phys. 3 (2012) 111.

[37] G. K.-L. Chan, M. Head-Gordon, Highly correlated calculations with a polynomial cost algorithm: A study of the density matrix renormalization group, J. Chem. Phys. 116 (2002) 4462.

[38] A. O. Mitrushenkov, R. Linguerri, P. Palmieri, G. Fano, Quantum chemistry using the density matrix renormalization group II, J. Chem. Phys. 119 (2003) 4148.

[39] O. Legeza, J. Sólyom, Optimizing the density-matrix renormalization group method using quantum information entropy, Phys. Rev. B 68 (2003) 195116.

[40] G. Moritz, B. A. Hess, M. Reiher, Convergence behavior of the density-matrix renormalization group algorithm for optimized orbital orderings, J. Chem. Phys. 122 (2005) 024107.

[41] J. Rissler, R. M. Noack, S. R. White, Measuring orbital interaction using quantum information theory, Chemical Physics 323 (2006) 519.

[42] S. Liang, H. Pang, Approximate diagonalization using the density matrix renormalization-group method: A two-dimensional-systems perspective, Phys. Rev. B 49 (1994) 9214.

[43] E. Cuthill, J. McKee, Reducing the bandwidth of sparse symmetric matrices, in: Proceedings of the 1969 24th national conference, ACM '69, ACM, New York, NY, USA, 157–172, 1969.

[44] W. M. Chan, A. George, A linear time implementation of the reverse Cuthill-McKee algorithm, BIT Numerical Mathematics 20 (1980) 8–14.

[45] S. W. Sloan, A FORTRAN program for profile and wavefront reduction, International Journal for Numerical Methods in Engineering 28 (1989) 2651.

[46] W. M. D. Center, Graph Utilities Package Tutorial, http://reference.wolfram.com/mathematica/GraphUtilities/tutorial/GraphUtilities.html, 2012.

[47] A. F. Albuquerque, F. Alet, P. Corboz, P. Dayal, A. Feiguin, S. Fuchs, L. Gamper, E. Gull, S. Gürtler, A. Honecker, R. Igarashi, M. Körner, A. Kozhevnikov, A. M. Läuchli, S. R. Manmana, M. Matsumoto, I. P. McCulloch, F. Michel, R. M. Noack, G. Pawlowski, L. Pollet, T. Pruschke, U. Schollwöck, S. Todo, S. Trebst, M. Troyer, P. Werner, S. Wessel, The ALPS project release 1.3: Open-source software for strongly correlated systems, J. Magn. Magn. Mater. 310 (2007) 1187, see also http://alps.comp-phys.org.

[48] E. R. Gagliano, C. A. Balseiro, Dynamical Properties of Quantum Many-Body Systems at Zero Temperature, Phys. Rev. Lett. 59 (1987) 2999–3002.

[49] O. Waldmann, Spin dynamics of finite antiferromagnetic Heisenberg spin rings, Phys. Rev. B 65 (2001) 024424.